J Mol Model (2013) 19:5489–5500
DOI 10.1007/s00894-013-2049-8

ORIGINAL PAPER

Some insights into the binding mechanism of the $GABA_A$ receptor: a combined docking and MM-GBSA study

Hong-Bo Xie · Yu Sha · Jian Wang · Mao-Sheng Cheng

Received: 21 June 2013 / Accepted: 21 October 2013 / Published online: 17 November 2013

Abstract Gamma-aminobutyric type A receptor ($GABA_AR$) is a member of the Cys-loop family of pentameric ligand gated ion channels (pLGICs). It has been identified as a key target for many clinical drugs. In the present study, we construct the structure of human $2\alpha_1 2\beta_2\gamma_2$ $GABA_AR$ using a homology modeling method. The structures of ten benzodiazepine type drugs and two non-benzodiazepine type drugs were then docked into the potential benzodiazepine binding site on the $GABA_AR$. By analyzing the docking results, the critical residues His102 (α_1), Phe77 (γ_2) and Phe100 (α_1) were identified in the binding site. To gain insight into the binding affinity, molecular dynamics (MD) simulations were performed for all the receptor–ligand complexes. We also examined single mutant $GABA_AR$ (His102A) in complexes with the three drugs (flurazepam, eszopiclone and zolpidem) to elucidate receptor–ligand interactions. For each receptor–ligand complex (with flurazepam, eszopiclone and zolpidem), we calculated the average distance between the C_α of the mutant residue His102A (α_1) to the center of mass of the ligands. The results reveal that the distance between the C_α of the mutant residue His102A (α_1) to the center of flurazepam is larger than that between His102 (α_1) to flurazepam in the WT type complex. Molecular mechanic-generalized Born surface area (MM-GBSA)-based binding free energy calculations were performed. The binding free energy was decomposed into ligand-residue pairs to create a ligand-residue interaction spectrum. The predicted binding free energies correlated well ($\mathbf{R}^2$=0.87) with the experimental binding free energies. Overall, the major interaction comes from a few groups around His102 (α_1), Phe77 (γ_2) and Phe100 (α_1). These groups of interaction consist of at least of 12 residues in total with a binding energy of more than 1 kcal mol^{-1}. The simulation study disclosed herein provides a meaningful insight into $GABA_AR$–ligand interactions and helps to arrive at a binding mode hypothesis with implications for drug design.

Keywords Gamma-aminobutyric acid type A receptors · Homology modeling · Molecular dynamics simulation · Molecular docking · Molecular mechanic-generalized Born surface area

Introduction

Gamma-aminobutyric type A receptors ($GABA_ARs$) can underlie fast inhibitory synaptic transmissions in the central nervous system and are members of the Cys-loop family of receptors, which also includes the nicotinic acetylcholine receptor (nAChR), the 5-hydroxytryptamine type 3 receptor ($5HT_3R$), the glycine receptor (GlyR), and gamma-aminobutyric type C receptor ($GABA_CR$) [1]. $GABA_ARs$ are multi-subunit chloride-permeable ion channels and have activities that can be controlled by binding gamma-aminobutyrics (GABAs). As targets of a variety of pharmacologically and clinically important drugs, including benzodiazepines, neuroactive steroids, anesthetics and convulsants, $GABA_ARs$ can modulate anxiety, learning and memory [2–5]. $GABA_ARs$ are formed as pentameric combinations of 19

Electronic supplementary material The online version of this article (doi:10.1007/s00894-013-2049-8) contains supplementary material, which is available to authorized users.

H.-B. Xie · Y. Sha (✉) · J. Wang · M.-S. Cheng (✉)
Key Laboratory of Structure-Based Drugs Design and Discovery of Ministry of Education, School of Pharmaceutical Engineering, Shenyang Pharmaceutical University, Shenyang 110016, People's Republic of China
e-mail: shayu@syphu.edu.cn
e-mail: mscheng@syphu.edu.cn

H.-B. Xie
College of Bioinformatics Science and Technology, Harbin Medical University, Harbin 150081, People's Republic of China

different (α1-6, β1-3, γ1-3, δ, ε, π, θ, ρ1-3) polypeptide subunits and display diverse biological functions [6–9]. Most native $GABA_A$Rs contain two α, two β and one γ or one δ subunit, and the majority of native receptors are of the $2\alpha_1 2\beta_2\gamma_2$ $GABA_A$R type.

Although $GABA_A$Rs have been studied for many years, there is still no high-resolution crystal structure available for any subtype of the $GABA_A$Rs because of difficulties in protein expression and the crystallization of membrane proteins. Thus, computational modeling has been utilized extensively to make crucial advances in understanding the structure and function of $GABA_A$Rs.

Recently, the structure of the activated homopentameric *Caenorhabditis elegans* glutamate-gated chloride channel was resolved and provides an excellent basis for modeling the structure of pentameric ligand gated ion channels (pLGICs) [10]. Thus far, this structure shares the highest known sequence identity with $GABA_A$R (33.4 %).

Multiple studies have identified residues that are involved in mediating the apparent binding affinity of benzodiazepine binding site ligands. Czajkowski et al. [11] measured the effects of 22 single cysteine mutations, which were introduced throughout the benzodiazepine binding site on the potentiation of I_{GABA} by flurazepam (FZM), eszopiclone (ESZ), and zolpidem (ZOP). They found that the residues that line the benzodiazepine binding site pocket most likely have different roles. For instance, some residues might interact directly with the ligand, while others might stabilize the structure of the binding site or mediate local conformational movements important for coupling benzodiazepine binding to the modulation of I_{GABA}.

In the present study, we applied homology modeling and molecular dynamic simulation methods to develop 3D molecular models of the $GABA_A$R based on the structure of the glutamate-gated chloride channel (GluCl) (PDB code: 3RHW) [12]. We used the structure of the $GABA_A$R to generate the hypothetical binding modes of ten classical benzodiazepine drugs and two non-benzodiazepine drugs. These drugs can all bind to the benzodiazepine binding site on the $2\alpha_1 2\beta_2\gamma_2$ $GABA_A$R, which mediates its therapeutic hypnotic properties [13–15]. Finally, we analyzed the interactions between key residues in the binding pocket and multiple ligands based on previous experiments.

Towards understanding the mechanism of benzodiazepine and non-benzodiazepine drugs in the binding site, we performed an extensive analysis of molecular dynamics simulations performed for all receptor-ligand complexes. Furthermore, single mutant His102A (α_1) $GABA_A$R molecular dynamics simulations were also performed for the complexes H102A-FZM, H102A-ESZ and H102A-ZOP to test the function of His102 (α_1) in the benzodiazepine binding site. We considered the way mutations affect the structure and compared common features between single mutant and wild-type (WT) $GABA_A$Rs. The energetic contributions of the residues in the benzodiazepine binding site were then assessed by performing molecular mechanics-generalized Born surface area (MM-GBSA) calculations on all the receptor–ligand complexes [16, 17]. Interactions between the drugs and each residue in the benzodiazepine binding site were analyzed using the MM-GBSA method to calculate the absolute binding free energies, which were further decomposed on a per-residue basis. The predicted binding free energies correlated well with the experimental binding free energies (R^2=0.87). The estimation of the binding free energy and its relative change (between WT and mutant) gives valuable information on drug–target relationships.

Computational details

Homology modeling

The sequences of the human $GABA_A$R α_1 (UniProt ID: P14867), β_2 (UniProt ID: P47870) and γ_2 (UniProt ID: P18507) subunits were retrieved from the ExPASy Molecular Biology Server (http://us.expasy.org). Recently, Hibbs and Gouaux [10] presented the first three-dimensional (3D) structure of an inhibitory anion-selective Cys-loop receptor (PDB ID: 3RHW), which shares sequence identity (33.4 %) with $GABA_A$R and can be used as a template for the $GABA_A$R receptor. Additionally, it should be noted that we did not construct the IC domain of the $GABA_A$R. It was difficult to build the IC domain because there was no suitable template to model this region, although it has been demonstrated that the IC domain can contribute to ion permeation [18, 19]. However, the IC domain has no effect on the benzodiazepine binding site because the two regions are a long distance apart and cannot interact with each other. To the best of our knowledge, no mutant experiments have yet demonstrated the influence of binding affinity of benzodiazepine drugs in the IC domain. Thus far, studies on drug binding affinity have focused only on the residues that line the benzodiazepine binding site pocket. Hence, here we discuss only the contribution of the ligand-binding site.

The sequences of the α_1, β_2, and γ_2 subunits were aligned to the corresponding subunits of the templates, as implemented using the Align Sequences protocol within the Discovery Studio 3.0 software package [20]. Twenty homology models were built and scored by the discrete optimized protein energy (DOPE) method [21]. Sigel et al. [22] previously demonstrated the absolute arrangement of the $\alpha_1\beta_2\gamma_2$ $GABA_A$R. Only one of these arrangements, which is shown in Fig. 1, was well accepted and thus chosen for our study. The quality of the constructed models was assessed with the Rampage server (http://www-cryst.bioc.cam.ac.uk). The structure of the mutant $GABA_A$R was prepared based on WT $GABA_A$R,

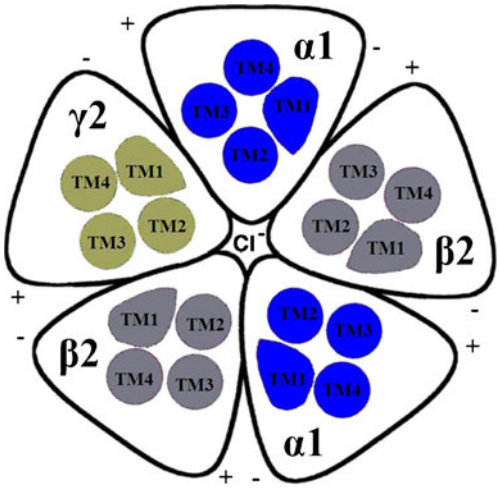

Fig. 1 The view from the synaptic cleft shows the absolute subunit arrangements of the $2\alpha_1 2\beta_2\gamma_2$ gamma-aminobutyric type A receptor ($GABA_AR$). The four transmembrane segments of each subunit are colored to illustrate the TM_2 segments lining the pore region of the channel. + (plus) and − (minus) refer to the asymmetric sides of the subunits

and the procedure was performed using the Build Mutants protocol with the Discovery Studio 3.0 software package.

Molecular docking

The classical binding pocket for benzodiazepines is located in a cleft between the α_1 and γ_2 subunits (Fig. 2). However, it is important to realize that these binding sites can interact not only with drugs that have a benzodiazepine structure but also some drugs with β-carboline, imidazopyridine, triazolopyridazine and cyclopyrrolone segments [23]. To explore the key residues of the benzodiazepine binding site of the $GABA_AR$, molecular docking of ten benzodiazepine and two non-benzodiazepine drugs to the $GABA_AR$ was performed using AutoDock 4.0 [24]. The model of the $GABA_AR$ was converted to PDBQT format using AutoDock Tools (ADT) version 1.5.4 (http://mgltools.scripps.edu). Then, Kollman united atom partial charges were assigned for the receptor. The grid size for the search space was set at 60 Å× 60 Å×60 Å, centered on the interface between the α_1 and γ_2 subunits, with a default grid point spacing of 0.375 Å. The Lamarckian genetic algorithm was used with a population size of 200 dockings and 25 million energy evaluations. The results were clustered according to the root-mean-square deviation (RMSD) criterion. Neither the highest ranking nor the lowest energy structures were used as the final result; instead, the final result was determined based on a combination of clustering, energy and interacting residue data, as shown in Supplementary data.

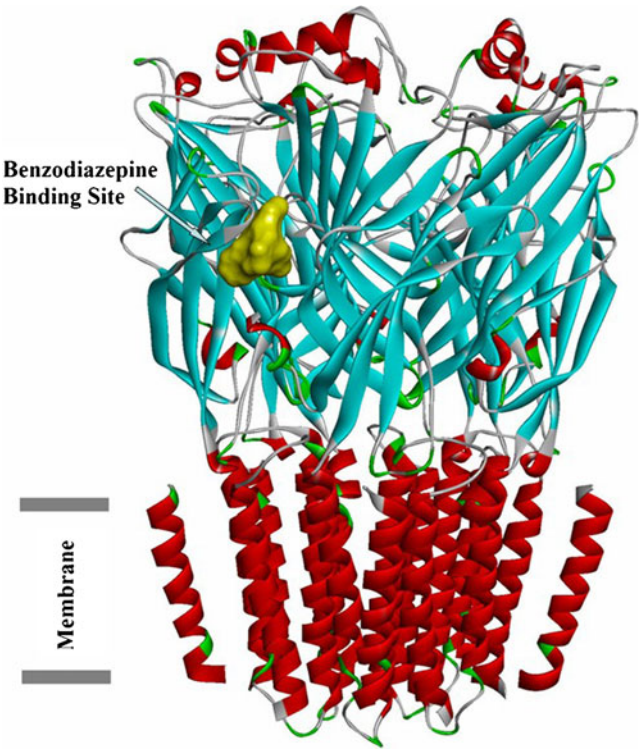

Fig. 2 View of the benzodiazepine binding site, looking parallel to the membrane

Molecular dynamics

Molecular dynamics simulations using Amber12 were performed to generate an ensemble of conformations for each receptor–ligand complex, followed by MM-GBSA calculations to estimate the binding free energy [25]. The Amber ff99SB force field was used in the system [26]. The empirical charge model AM1-BCC generated the ligands' atomic partial charges by using the Antechamber module in AmberTools 12 [26, 27]. Each complex was solvated in a TIP3P water box with a minimum distance of 8 Å from the surface of the complex to the edge of the simulation box. Each system was neutralized by adding Na^+ or Cl^- ions.

The solvated complex was subject to an initial energy minimization with solute restraint followed by a complete minimization without restraint. Each energy minimization consisted of a 5,000-step steepest descent minimization followed by another 1,000-step conjugated gradient. Subsequently, a 100-ps MD simulation was performed with the complex subject to positional restraint. The 100-ps MD simulation was used to heat the system from 0 to 300 K in NVT ensemble. Finally, a 10-ns unrestrained NPT simulation was performed, with temperature and pressure controlled at 300 K and 1 atm, respectively, by applying the Berendsen weak-coupling algorithm [28]. The particle mesh Ewald (PME) method was used to treat long-range electrostatic interactions [29]. The cut-off distances for the real space of PME and the van der Waals interactions were set to 10 Å. All bonds involving hydrogen atoms were constrained using the SHAKE algorithm [30].

The binding free energies of the receptor–ligand complexes were calculated by the MM-GBSA method. In this method the binding free energy, ΔG_{bind}, is calculated as the sum of MM energy, ΔE_{MM} with the solvation free energy contribution to binding, ΔG_{sol} and the conformational entropic contribution, $-T\Delta S$. This can be represented as $\Delta G_{bind}=\Delta E_{MM}+\Delta G_{sol}-T\Delta S$; where both ΔE_{MM} and ΔG_{sol} can be divided into two parts: $\Delta E_{MM}=\Delta E_{ele}+\Delta E_{vdw}$; $\Delta G_{sol}=\Delta G_{gb}+\Delta G_{np}$, where ΔE_{ele} and ΔE_{vdw} are the electrostatic interaction and van der Waals (vdw) energy in the gas phase and ΔG_{gb} and ΔG_{np} are the polar and non-polar contributions to the solvation free energy, respectively. The polar contribution of the solvation energy (ΔG_{gb}) was calculated using the GB model, in which the parameters were developed by Onufriev et al [31]. $-T\Delta S$ is generally calculated using classical statistical thermodynamics and normal mode analysis.

Results and discussion

Validation of the homology models

The homology models were validated using the Rampage server. Ninety-five percent of the residues were found in the favored regions of the Ramachandran plot, and 4 % of the residues reside were in the accepted regions (Fig. 3). This suggested that the homology model structure had a satisfactory geometry and could be used for further MD simulation studies. The template used to model the $GABA_AR$ was GluCl, which had a high sequence identity to $GABA_AR$, especially in loop B, loop E, TM_1, and TM_2 as shown in Fig. 4. The following residues were conserved and have been identified with site-specific mutagenesis experiments: Phe100 (α_1), Arg144 (γ_2), Thr261 (α_1) and Thr255 (β_2) [32–34].

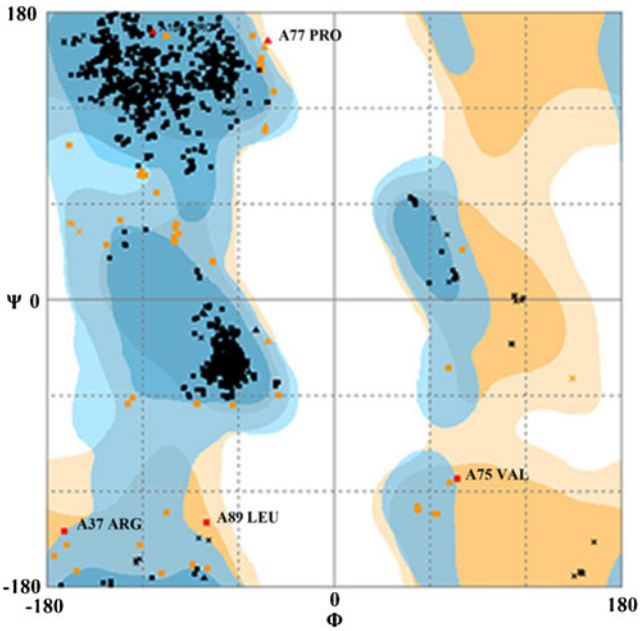

Fig. 3 Ramachandran plot of the $GABA_AR$. A total of 95.5 % of the residues fall in the favorable areas, and 4 % of the residues reside in allowed areas

Molecular docking

Docking study of benzodiazepine drugs

Two clusters of FZM docking poses were obtained (Supplementary Fig. S2–S4, Table S1). Cluster 2 had the most docking conformations of FZM and a key residue His102 (α_1) formed a hydrogen bond with FZM. Therefore, we chose it as the best docking pose of FZM. FZM was found docked into the binding pore regions of $GABA_AR$ and surrounded by Lys156 (α_1), Val203 (α_1), Val212 (α_1), Tyr210 (α_1), His102 (α_1), Tyr160 (α_1), Asn60 (γ_2), Phe77 (γ_2), Phe100 (α_1), Tyr58 (γ_2). The orientation of the ligand was observed to favor its stability, which is required for interaction with the receptor. The adjacent His102 (α1) was in a good position to interact with the N atom of the seven-membered ring in FZM via hydrogen bonds. As observed in the 3D model of FZM with $GABA_AR$, which is depicted in Fig. 5a, four residues interact directly with the ligand via hydrophobic contacts. These contacts are between (1) the benzene ring and Val203 (α_1), Phe77 (γ_2), and (2) the N, N-diethylethanamine moiety and Phe100 (α_1), Val212 (α_1). According to the docking results of each benzodiazepine drug, we found that the ten drugs shared the same binding mode. First, the orientation of the skeleton structures 2,3-dihydro-1*H*-benzo[e][1, 4]diazepine was highly semblable. Second, the interactions between the receptor and ligands were very similar. To give a clear explanation, a detailed view of docked benzodiazepine drugs with the binding pocket of $GABA_AR$ is given in Fig. S1. The nitrogen atom of acrylamide as the hydrogen bond acceptor was hydrogen-bonded with His102 (α_1). The phenyl groups all point to Ala161 (α_1). All of the above indicated the good predictive ability of the docking model.

Docking study of non-benzodiazepine drugs

Three clusters of ESZ docking poses were obtained (Supplementary Fig. S5–S8, Table S2). We chose cluster 1 as the final docking pose of ESZ because it had the most docking poses and the lowest docked energy. The docking study performed for ESZ suggests that the oxygen atom of its carbonyl group was hydrogen-bonded to Ser205 (α_1), and the predicted H-bond distance was 2.76 Å. The N atom of the pyrazine ring in the structure was also hydrogen-bonded to residue Thr207 (α_1). Met130 (γ_2), Phe77 (γ_2), and Val203 (α_1) were also located within 5 Å of ESZ; however, these three residues were involved in hydrophobic contacts rather than hydrogen-bonding interactions. As mentioned above, hydrophobic interactions were also

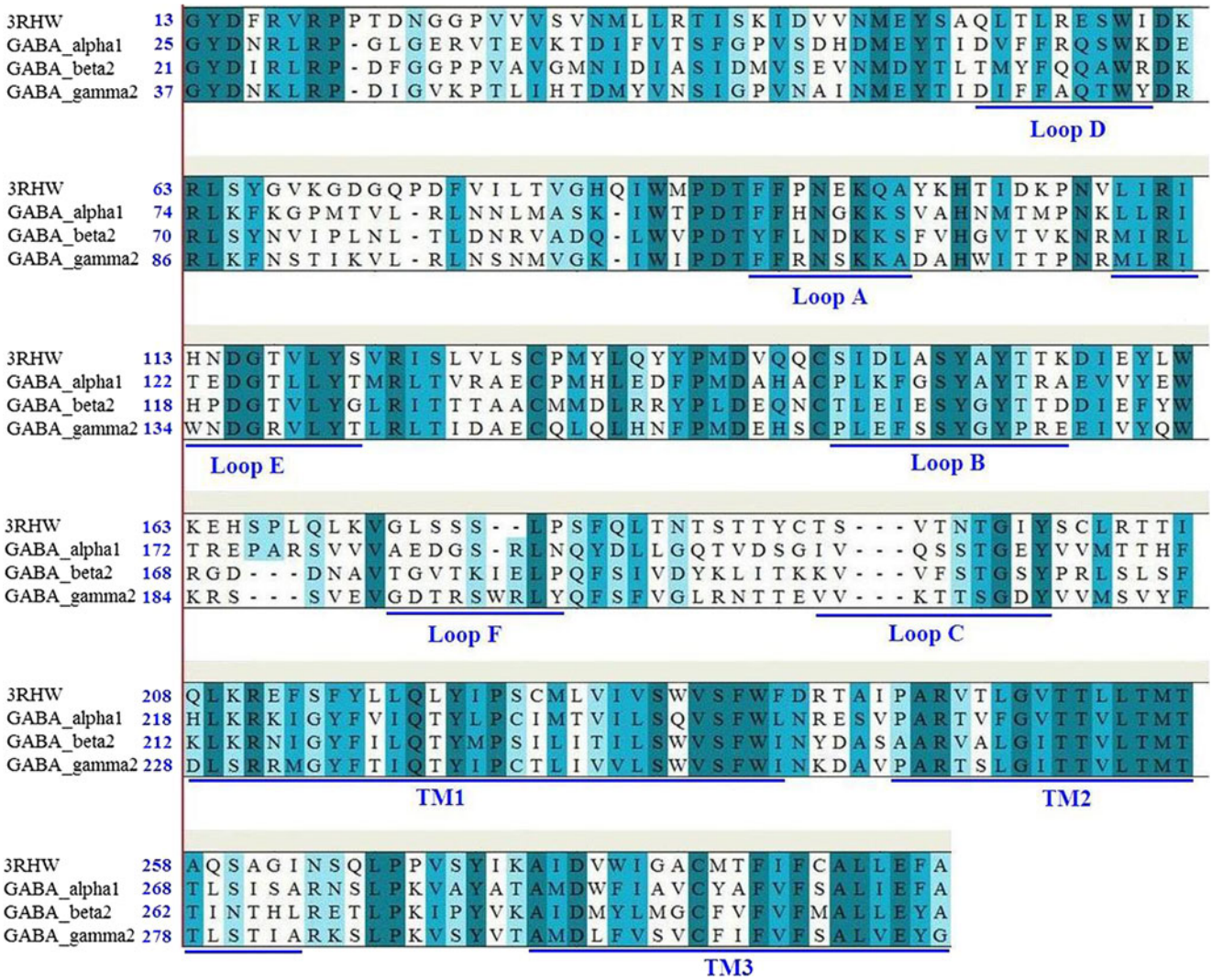

Fig. 4 Target sequences ($GABA_AR$ α_1, β_2 and γ_2 subunits) are aligned with the template sequence (GluCl 3RHW). The deeper the color of the residues, the higher the sequence identity

identified between Phe77 (γ_2), Val203 (α_1) and FZM; thus, it was obvious that these residues played significant roles in benzodiazepine binding. More importantly, ESZ is a chiral compound and is responsible for all the desired effects, while the other enantiomer seems to be inactive. Fig. 5b shows that the chiral chain 4-methylpiperazine has a hydrophobic interaction with Phe77 (γ_2); thus, we inferred that Phe77 (γ_2) is a crucial residue for the selective activity of ESZ.

Four clusters of ZOP docking poses had more than ten conformations (Supplementary Fig. S9–S13, Table S3). Thus far, many mutagenic data showed that His102 (α_1) is an essential recognition site point for zolpidem. Therefore, cluster 2 was chosen as the best docking pose because it is the only cluster that has a hydrogen bond with His102 (α_1). ZOP binds with high affinity and acts as a full agonist for the α_1-containing $GABA_AR$ and approximately 10-fold lower affinity for α_2- or α_3-containing $GABA_AR$ isoforms [35]. To date, many docking studies have been performed to illustrate the binding mode of ZOP with $GABA_AR$ [36, 37]. In this study, to gain insights into the potential interactions between ZOP and $GABA_AR$, we evaluated all residues within 5 Å of the ligand. A 3D model of ZOP in the active pocket is shown in Fig. 5c. The only carbonyl group of the ligand was rotated considerably to accommodate H-bonding to the amino group of His102 (α_1). Additionally, most of the residues around ZOP were involved in hydrophobic contacts, including Val203 (α_1), Val212 (α_1), Met130 (γ_2), Phe100 (α_1), and Phe77 (γ_2).

Comparison with data from mutagenesis experiments

In summary, the docking results provide new insights into the roles of some conserved residues in the binding of six typical agonists to human $\alpha_1\beta_2\gamma_2$ $GABA_AR$. These data will be helpful in the design of novel agonists for $GABA_ARs$. As

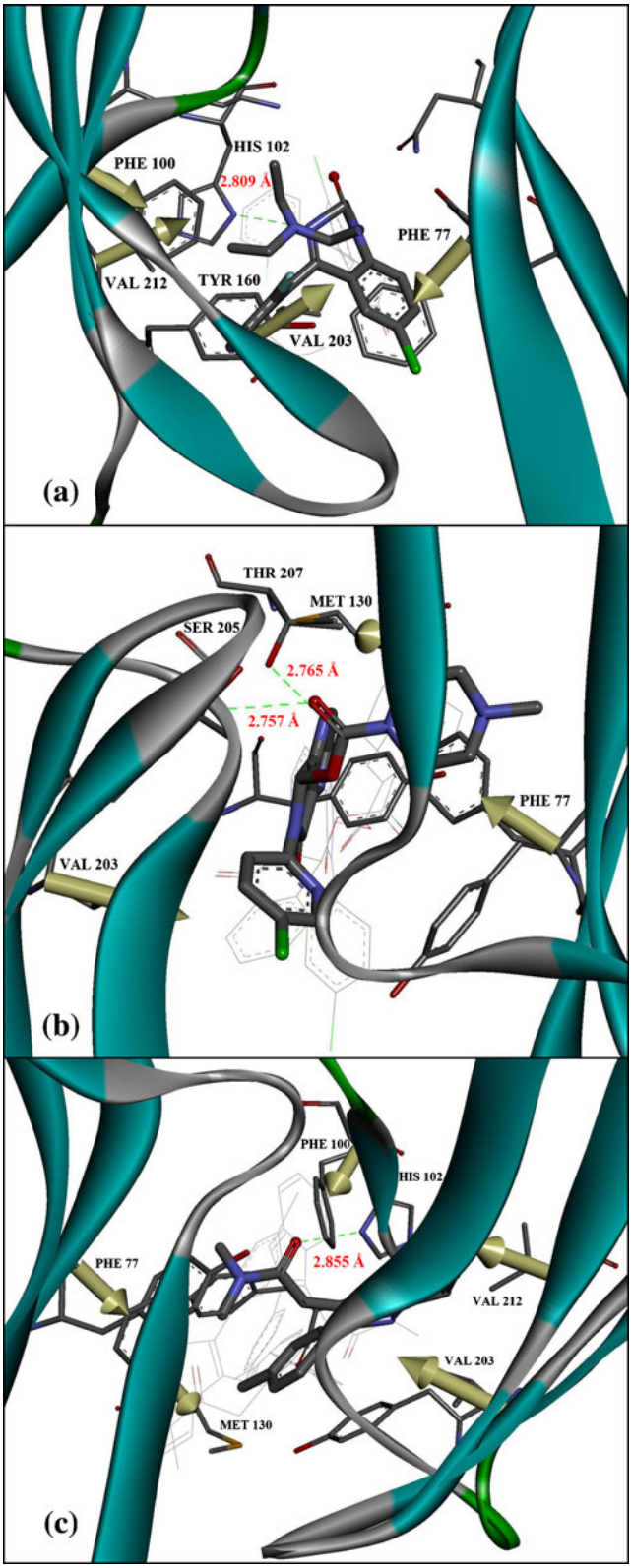

Fig. 5a–c The putative agonist binding site is represented in ribbon form, and ligands are shown as stick representation, colored by element. Other cluster docking poses are shown with wire frames to indicate the degree of variability in the docking procedure. **a** Docked flurazepam (FZM) with $GABA_AR$. **b** Docked eszopiclone (ESZ) with $GABA_AR$. **c** Docked zolpidem (ZOP) with $GABA_ARFZM$

shown by these results, His102 (α_1) and Phe77 (γ_2) were the most critical residues, while residues Val203 (α_1), Val212 (α_1), Met130 (γ_2), and Phe100 (α_1) were also important binding determinants that had strong hydrophobic interactions with the ligands. Therefore, we should take special note of those ligands that interact with the above residues in virtual drug screening. In comparing our results with results from site-directed mutagenesis experiments, we found that several key residues in our docking predictions were relevant to previous studies. In biological experiments, Phe100 (α_1), Phe77 (γ_2), and His102 (α_1) were identified as important residues for benzodiazepines binding [11, 38, 39]. Furthermore, Thr207 (α_1) and Phe77 (γ_2) can also interact with ESZ. Phe100 (α_1), Val212 (α_1), His102 (α_1), Met130 (γ_2), and Phe77 (γ_2) played important roles in the inhibition of ZOP [11, 40–42]. In our docking study, Met130 (γ_2) had a hydrophobic interaction with ZOP; however, Morlock and Czajkowski [11] reported that Met130 (γ_2) was not a key residue for the inhibition of ZOP, which partly contradicted the results of Sigel's experiments [40–42]. Additionally, we found that Ser205 (α_1) formed a hydrogen bond with ESZ. Although the mutant $\alpha_1S205C\beta_2\gamma_2$ $GABA_AR$ could decrease ESZ potentiation compared with the wild type (WT) $GABA_AR$, this effect was small. In Czajkowski's study [11], the ESZ maximal potentiation of I_{GABA} with $\alpha_1S205C\beta_2\gamma_2$ was 1.7±0.2; the ESZ maximal potentiation of I_{GABA} with WT $GABA_AR$ was 2.8±0.3, where the maximal potentiation was calculated as $[(I_{GABA + ESZ}/I_{GABA}) - 1]$. However, only a few site-directed mutagenesis studies have investigated the inhibition of ESZ, so we could not obtain more information about this residue. It is normal for experimental data collected in different systems to contain some discrepancies. Thus, additional experiments should be conducted for these three drugs to assess our docking results. Moreover, depending on the ligands, the effects of some mutations were different, indicating that the structural mechanisms underlying the ability of ligands to interact with divergent structures are distinct. Details of the comparisons of our docking study with experimental data have been listed in Table 1. Overall, these comparisons confirmed the reliability of our homology modeling and docking results.

Molecular dynamics

Stability of trajectories

Here, we describe 15 MD simulation systems, including 12 WT receptor-ligand complexes and 3 mutant receptor-ligand complexes. The simulation time was 10 ns each for all ligand–receptor complexes, which allowed us to extract reliable conformational and functional features of the benzodiazepine binding site of the $GABA_AR$. As an indicative measure of the stability and conformational drift of the proteins in the

Table 1 Key residues in docking studies and mutagenesis experiments

Ligand	Docking results	Mutagenesis in Reference
FZM	His102 (α1) Phe77 (γ_2)	Phe100 (α_1) [11]
	Phe100 (α_1) Val203 (α_1)	Phe77 (γ_2) [38]
	Val212 (α_1)	His102 (α1) [39]
ESZ	Ser205 (α_1) Thr207 (α_1) Phe77 (γ_2) Val203 (α_1)	Thr207 (α_1) [11]
	Met130 (γ_2)	Phe77 (γ_2) [40]
ZOP	His102 (α_1) Val203 (α_1)	Val212 (α_1) Phe100 (α_1) His102 (α_1) [11]
	Val212 (α_1) Met130 (γ_2)	Met130 (γ_2) [41]
	Phe100 (α_1) Phe77 (γ_2)	Phe77 (γ_2) Met130 (γ_2) [42]

simulations, the RMSDs of the backbone atom coordinates from their initial values were monitored as a function of simulation time. The RMSD values of the $GABA_AR$ reached a plateau within the first 4 ns of the simulation (Fig. 6). This result signifies that the RMSD of all complexes were similar from the starting structures during the course of simulations, with values approximately 2 Å to 3.5 Å, ensuring stable trajectories. The RMSD plots indicate that the conformations of the WT and single mutant His102A (α_1) complexes are in good equilibrium.

To obtain the receptor–ligand interactions, we followed a simple method of calculating the average distance between the C_α of a key residue His102 (α_1) to the center of mass of the three agonists (FZM, ESZ and ZOP). In the H102A-ligand complexes, we calculated the average distance between the C_α of the mutant residue His102A (α_1) to the center of mass of the three agonists (FZM, ESZ and ZOP). A time-series plot for the interactions showed that the six trajectories run parallel to each other and ranged from 6 Å to 12 Å (Fig. 7). The result shows all three agonists fit properly and are accommodated well inside the binding site cavity in each of the complexes. The distance between the C_α of the mutant residue His102A (α_1) to the center of FZM is larger than that between His102 (α_1) to FZM in WT type complex, which might be the factor for the change of binding energy in the two complexes.

On the other hand, stable interactions were not observed between FZM and mutant His102A (α_1). This suggests that the interaction between FZM and His102 (α_1) might stabilize the binding mode. During the course of the MD simulation for $GABA_AR$-FZM, the phenyl group from FZM moves towards residues Ala161 (α_1) and Val212 (α_1), which form hydrophobic interactions. This is a fairly stable interaction and seems to help lock the molecule in place. Also the protein residues near the binding site close up around the benzodiazepines and partially bury them.

Binding free energy calculation for WT and mutant complexes

Free energy simulations predict conformational domains involved in receptor–ligand interactions using the MM-GBSA

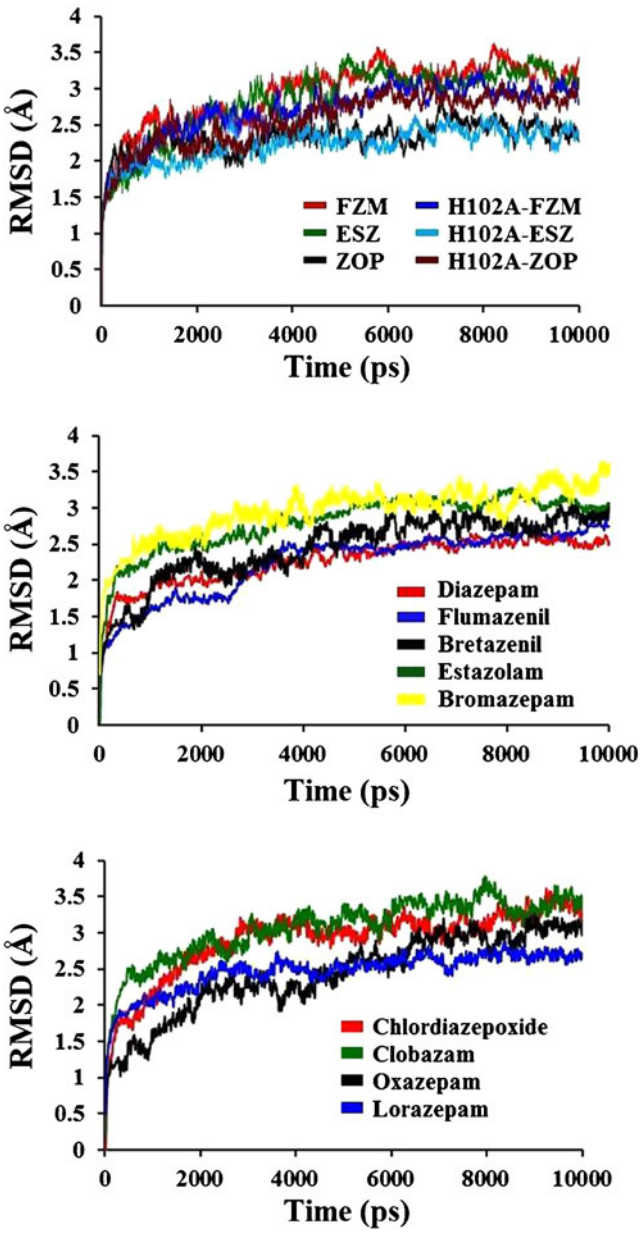

Fig. 6 Root-mean-square deviation (RMSD) plot for backbone Cα atoms relative to their initial minimized complex structures as a function of time

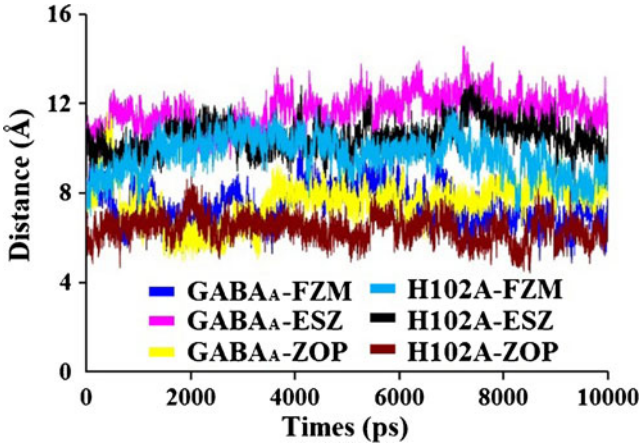

Fig. 7 Time-series plot of ligands distance for WT and H102A mutant simulations of the receptor–ligand complexes

calculation. As shown in Table 2, the calculated binding free energies with the contribution of the entropy was found to be −11.28 kcal mol^{-1} for GABA$_A$R-FZM, −10.08 kcal mol^{-1} for GABA$_A$R-ESZ, and −10.11 kcal mol^{-1} for GABA$_A$R-ZOP. This suggests that the binding free energy of FZM for the receptor–ligand complex is considerably higher than the binding affinities of ESZ and ZOP to WT GABA$_A$R. The results for the WT complexes agree with the available experimental affinities.

A breakdown of the different free energy components described in Table 2 for the three WT complexes and Table S4–S6 for the other benzodiazepine drugs revealed that the electrostatic component of enthalpy of solvation (ΔG_{gb}) contributed unfavorably to binding ($\Delta G>0$) for all three agonists, while ΔE_{ele}, which is the interaction energy due to electrostatic interactions between the receptor and agonists, led to favorable binding; however, the data showed that the non-polar component, ΔG_{np}, systematically contributed favorably ($\Delta G<0$) as expected because the formation of complexes reduced the solvent accessible surface area (SASA). These results suggest the molecular mechanical component of the free energy of binding between the three agonists and GABA$_A$R is the dominant factor promoting stability. In all three GABA$_A$R-ligand complexes, the intermolecular van der Waals interactions (ΔE_{vdw}) make the most significant contribution to the binding free energies, whereas the overall electrostatic interaction energies (ΔE_{ele}) are positive and unfavorable for the binding free energies.

Comparisons of the free energy components between the WT complexes and the mutant complexes were carried out to elucidate the interaction mechanism. In accordance with the energy components of the binding free energy shown in Tables 2 and 3, the van der Waals energies in the gas phase provided the dominant favorable contributions for the binding of all six receptor-ligand complexes. Non-polar solvation energies (ΔG_{np}) resulting from the interment of the SASA of all three ligands also have similar small favorable contributions to the binding affinity in all cases. Conversely, polar solvation energies (ΔG_{gb}) of the GABA$_A$R and entropy components (−TΔS) brought about an unfavorable contribution to their binding.

The MM-GBSA results revealed the impact of mutations on the binding affinity of FZM, ESZ and ZOP to His102A (Table 3). Our calculations supported His102A being a major mutation for FZM, as it had a reduced binding energy compared to the GABA$_A$R-FZM complex ($\Delta\Delta G_{bind}$= 6.35 kcal mol^{-1}, $\Delta\Delta G_{bind}$ is the difference between the binding free energy for WT and mutant receptor–ligand complexes). By decreasing the potential for hydrogen bond formation inside the binding cavity, FZM might not be bound as effectively. On the other hand, the His102A mutation did not greatly affect the binding of the ESZ and ZOP, although the lowest impact was observed in the single mutant His102A,

Table 2 Binding free energies (kcal mol^{-1}) of the wild-type receptor-ligand complexes. *FZM* Flurazepam, *ESZ* eszopiclone, *ZOP* zolpidem, *SD* standard deviation

	FZM		ESZ		ZOP	
	WT	SD	WT	SD	WT	SD
ΔE_{ele}	−7.64	2.25	−22.74	3.48	−6.13	3.46
ΔE_{vdw}	−46.34	2.33	−43.47	2.31	−35.71	2.15
ΔG_{gb}	22.71	1.17	39.96	3.66	18.06	3.05
ΔG_{np}	−5.27	0.29	−4.93	0.35	−4.38	0.19
ΔE_{MM}	−53.98	3.42	−66.21	4.45	−41.84	3.53
ΔG_{sol}	17.44	1.62	35.03	3.61	13.68	2.11
ΔG_{total}	−36.54	3.18	−31.18	3.76	−28.16	2.37
-TΔS	25.26	9.37	21.1	6.17	18.05	8.09
ΔG_{bind}	−11.28		−10.08		−10.11	
ΔG_{exp}	−10.64		−10.24		−10.26	

Table 3 Binding free energies (kcal mol^{-1}) of mutant receptor–ligand complexes

	FZM		ESZ		ZOP	
	H102A	std	H102A	std	H102A	std
ΔE_{ele}	−6.93	2.26	−13.16	3.18	−13.30	2.17
ΔE_{vdw}	−39.80	1.17	−47.36	2.33	−34.72	1.46
ΔG_{gb}	20.12	2.44	33.36	2.28	24.53	1.76
ΔG_{np}	−4.40	0.26	−5.17	0.19	−4.40	0.25
ΔE_{MM}	−46.73	3.03	−60.52	3.07	−48.02	2.55
ΔG_{sol}	15.72	2.27	28.19	2.18	20.13	1.41
ΔG_{total}	−31.01	2.09	−32.33	2.35	−27.89	2.61
-TΔS	26.08	9.25	23.78	7.21	19.07	8.88
ΔG_{bind}	−4.93		−8.55		−8.82	
$\Delta\Delta G_{bind}$	6.35		1.53		1.29	

with a binding energy of −8.55 kcal mol^{-1} for ESZ ($\Delta\Delta G_{bind}$=1.53 kcal mol^{-1}) and a binding energy of −8.82 kcal mol^{-1} for ZOP ($\Delta\Delta G_{bind}$=1.29 kcal mol^{-1}). The entropy term (−TΔS) was slightly higher for the three mutant H102A-ligand complexes; it was still close to the relevant WT $GABA_AR$-ligand complexes. In order to evaluate quantitatively the difference of the affinities of the studied drugs to $GABA_AR$, the MM-GBSA method was used to calculate the binding free energy for each complex. The correlation between the predictions of MM-GBSA with the experimental binding free energies is R^2=0.87

(Fig. 8. Table 4). This suggests that MM-GBSA has as good a capability to rank the bioactivities as molecular docking. We observe that the calculated free energy results have the same trend as the experimental inhibition constant *K*i values [13–15, 43–47].

Free-energy decomposition analysis

The interaction between the ligands and each $GABA_AR$ residue was computed using the MM-GBSA decomposition process applied in the mm-pbsa module in AMBER12. The binding interaction of each inhibitor-residue pair includes four terms: van der Waals (ΔE_{vdw}) contribution and electrostatic (ΔE_{ele}) contribution (in the gas phase), polar solvation (ΔG_{pol}) contribution, and nonpolar solvation (ΔG_{nopol}) contribution.

$$\Delta G_{inhibitor-residue} = \Delta E_{vdw} + \Delta E_{ele} + \Delta G_{pol} + \Delta G_{nopol}$$

The polar contribution (ΔG_{pol}) to solvation energy was calculated using the generalized Born (GB) module. All energy components were calculated using 50 snapshots from the last 2.0 ns of the MD simulation.

To characterize the different contributions to the binding free energies of FZM, ESZ and ZOP with WT $GABA_AR$ and mutant $GABA_AR$, absolute binding free energies were calculated for the six complexes by the MM-GBSA method. The binding free energy was decomposed into ligand-residue pairs to generate a ligand-residue interaction spectrum. As seen in Fig. 9, the contribution of individual residue to binding varies from +0.3 to −4.0 kcal mol^{-1}. These groups of interaction consist at least of 12 residues in total with the binding energy of more than 1 kcal mol^{-1}. The decomposition approach was helpful for locating residues that contribute to the receptor–ligand interaction.

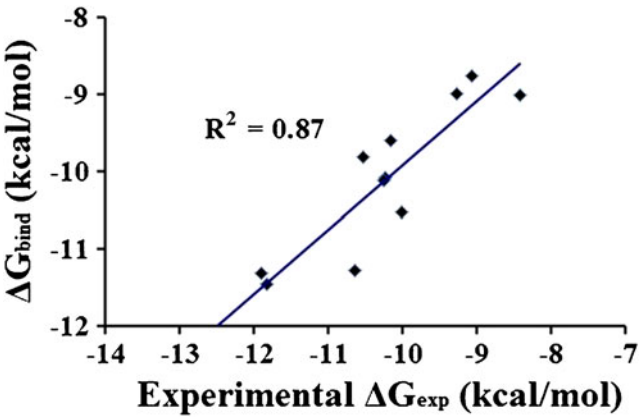

Fig. 8 Correlation of the predicted binding energies by molecular mechanic-generalized Born surface area (MM-GBSA) with available experimental binding energies

Table 4 Experimental *K*i values and binding free energies predicted by the molecular mechanic-generalized Born surface area (MM-GBSA) method

Compound	Predicted ΔG_{bind} (kcal mol^{-1})	*K*i (nM)[a]	ΔG_{exp} (kcal mol^{-1})[b]
Flurazepam	−11.28	16 [13]	−10.63
Diazepam	−8.98	160 [45]	−9.27
Estazolam	−9.81	19 [46]	−10.53
Flumazenil	−11.31	1.9 [43]	−11.90
Bretazenil	−12.80	0.16 [45]	−13.36
Bromazepam	−10.53	45 [44]	−10.02
Chlordiazepoxide	−9.01	670 [47]	−8.42
Clobazam	−8.76	222 [44]	−9.08
Oxazepam	−9.61	36 [46]	−10.15
Lorazepam	−11.45	2.1 [45]	−11.83
Eszopiclone	−10.08	31 [15]	−10.24
Zolpidem	−10.11	30 [14]	−10.26

[a] Experimental *K*i values are taken from the references noted

[b] ΔG_{exp}=−RTln(*K*i), where the temperature *T* is determined as 298.15 K

For FZM, ESZ and ZOP, the major binding attractions come from the residues Phe100 (α_1), His102 (α_1) and Phe77 (γ_2). This phenomenon can be explained by the fact that His102 (α_1) hydrogen bonds to FZM and ZOP. Phe100 (α_1) and Phe77 (γ_2) are the important amino acids that make the greatest contributions to the binding affinities. The main force for amino acid Phe100 (α_1) and Phe77 (γ_2) is the van der Waals energy, which also predominantly drives the binding of the drug to Val212 (α_1) and Met130 (γ_2) in the $GABA_AR$-ZOP complex. Arg144 (γ_2), Ser205 (α_1) and Thr207 (α_1) are all important residues in the $GABA_AR$-ESZ complex. The total contribution from polar salvation energies and electrostatic energy is the key driving force for the binding of ESZ to these residues. Morlock and Czajkowski [11] have identified that these residues might directly interact with the ligand and stabilize the structure of the binding site and contribute to benzodiazepine binding affinity; His102 (α_1) mediates local conformational movements important for coupling ligand binding to the modulation of I_{GABA}.

A subsequent analysis of the separate energy terms contributing to the MM-GBSA free energy suggested that

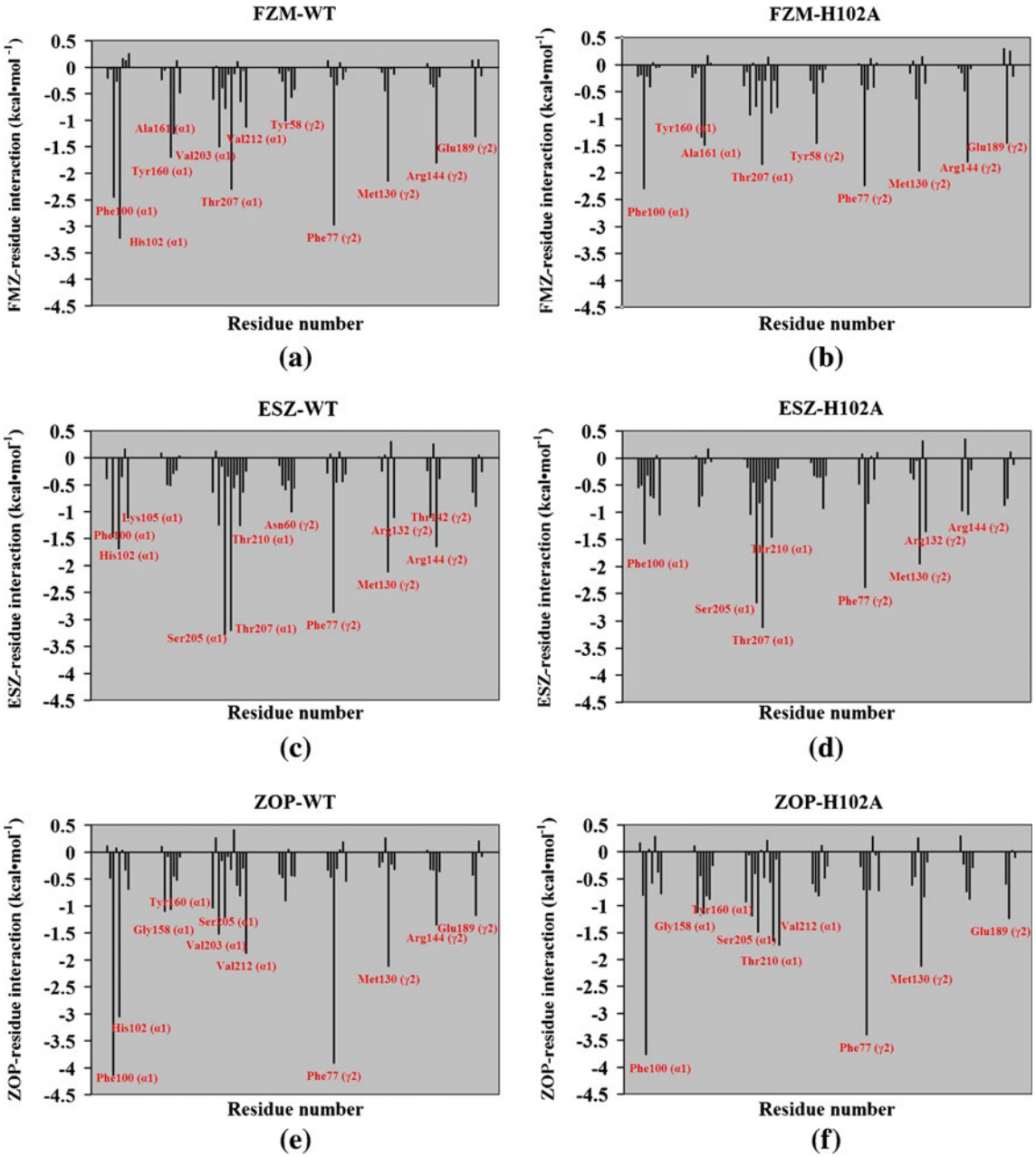

Fig. 9a–f Decomposition of ΔG on a per-residue basis for the ligand-GABA$_A$R complex. **a** FMZ-WT, **b** FMZ-H102A, **c** ESZ-WT, **d** ESZ-H102A, **e** ZOP-WT, **f** ZOP-H102A

favorable Van der Waals and nonpolar interactions mainly drive the association between GABA$_A$R and each agonist. Specifically, amino acids Phe100 (α_1), His102 (α_1), Phe77 (γ_2), Val212 (α_1) and Met130 (γ_2) were found to be responsible for the high affinity interaction, as observed when separating the binding free energy into individual components.

The binding free energy decomposition analysis also demonstrates an obvious reduction of the energy contribution of residue His102A (α_1) in the mutant complexes. Apart from the variation in His102A (α_1), the contribution of residue Arg144 (γ_2) is also reduced substantially in ESZ and ZOP complexes. According to the energy decomposition results, the energy reduction of Arg144 (γ_2) results mainly from the impact of the polar interactions ($\Delta E_{ele}+\Delta G_{gb}$), which indicates that even subtle alterations of ligand geometry can produce profound differences in electrostatic interactions.

Conclusions

In the absence of a crystal structure of GABA$_A$R, we constructed a 3D model of the human $2\alpha_1 2\beta_2\gamma_2$ GABA$_A$R.

Molecular docking of two sets of ligands for the $GABA_AR$ was also performed in this study. The results of docking in the $GABA_AR$ revealed the main differences in the binding modes of these ligands and the critical residues that are involved in the recognition of the agonists. There are three important residues in the benzodiazepine binding site: His102 (α_1), Phe77 (γ_2), and Phe100 (α_1). His102 (α_1) can form hydrogen bonds with benzodiazepine drugs and ZOP, and the other residues were clearly involved in hydrophobic interactions. These results were all confirmed by comparisons with previous biological experiments. Hence, future studies should focus on these residues to design new potential agonists for $GABA_AR$.

In this study, we used a series of molecular modeling techniques, including conventional MD simulations, MM-GBSA binding free energy predictions, and MM-GBSA binding free energy decomposition analysis, to explore the impact of one mutation in the benzodiazepine binding site. The predicted binding free energies of ten benzodiazepine drugs and two non-benzodiazepine drugs to the WT complexes are consistent with the experimental data. Results of both MM-GBSA calculations give the correct order in which to rank the inhibitory potency of the studied systems: WT>His102A (α_1). The binding mode of the binding site was quite stable around the molecule. The MM-GBSA-based free energy calculations showed that the FZM bound with greater specificity than the other two non-benzodiazepine drugs (ESZ and ZOP) to the $GABA_AR$. Moreover, our computational simulations demonstrate that the mutation of His102A (α_1) has a great influence on the benzodiazepine binding site, and the variations in polar interactions, involving primarily the residues His102 (α_1), Phe77 (γ_2), and Phe100 (α_1), which play critical roles in the development of drug resistance. We demonstrated that the structural determinants for high-affinity binding of ESZ and FZM are different. We can envision that, depending on the orientation of the ligands in the binding pocket and their contact residues, some of the residues involved in the initial coupling of binding might differ. ESZ binding is dependent largely on shape recognition; Ser205 and Thr207 might cause ESZ to prefer a position that has a greater efficacy.

In accordance with the energy components of the binding free energy, the van der Waals energies provided the dominant contribution to ligand binding for all WT $GABA_AR$-ligand complexes. In the absence of an experimentally determined structure for $\alpha_1\beta_2\gamma_2$ $GABA_AR$, our model will be valuable for further biochemical and pharmacological studies concerning the detailed structure of the protein and other subtypes of $GABA_ARs$.

Acknowledgments This study is supported by the Program for Innovative Research Team of the Ministry of Education and Program for Liaoning Innovative Research Team in University.

References

1. Absalom NL, Schofield PR, Lewis TM (2009) Pore structure of the Cys-loop ligand-gated ion channels. Neurochem Res 34(10):1805–1815
2. Pritchett DB, Sontheimer H, Shivers BD, Ymer S, Kettenmann H, Schofield PR, Seeburg PH (1989) Importance of a novel GABAA receptor subunit for benzodiazepine pharmacology. Nature 338(6216):582–585
3. Sieghart W, Sperk G (2002) Subunit composition, distribution and function of GABA(A) receptor subtypes. Curr Top Med Chem 2(8):795–816
4. Johnston GA (2005) GABA(A) receptor channel pharmacology. Curr Pharm Des 11(15):1867–1885
5. Mehta AK, Ticku MK (1999) An update on GABAA receptors. Brain Res Brain Res Rev 29(2–3):196–217
6. Davies PA, Hanna MC, Hales TG, Kirkness EF (1997) Insensitivity to anaesthetic agents conferred by a class of GABA(A) receptor subunit. Nature 385(6619):820–823
7. Korpi ER, Sinkkonen ST (2006) GABA(A) receptor subtypes as targets for neuropsychiatric drug development. Pharmacol Ther 109(1–2):12–32
8. Rudolph U, Crestani F, Mohler H (2001) GABA(A) receptor subtypes: dissecting their pharmacological functions. Trends Pharmacol Sci 22(4):188–194
9. Sarto-Jackson I, Sieghart W (2008) Assembly of GABA(A) receptors (Review). Mol Membr Biol 25(4):302–310
10. Hibbs RE, Gouaux E (2011) Principles of activation and permeation in an anion-selective Cys-loop receptor. Nature 474(7349):54–60
11. Morlock EV, Czajkowski C (2011) Different residues in the GABAA receptor benzodiazepine binding pocket mediate benzodiazepine efficacy and binding. Mol Pharmacol 80(1):14–22
12. Xie HB, Wang J, Sha Y, Cheng MS (2013) Molecular dynamics investigation of Cl transport through the closed and open states of the 2alpha2betagamma GABA receptor. Biophys Chem 180–181C:1-9.
13. Nestoros JN (1982) Benzodiazepine and gaba receptors are functionally related: further electrophysiological evidence in vivo. Prog Neuropsychopharmacol Biol Psychiatry 6(4–6):417–420
14. McLeod M, Pralong D, Copolov D, Dean B (2002) The heterogeneity of central benzodiazepine receptor subtypes in the human hippocampal formation, frontal cortex and cerebellum using [3H]flumazenil and zolpidem. Brain Res Mol Brain Res 104(2):203–209
15. Blanchard JC, Boireau A, Julou L (1982) Brain receptors and zopiclone. Int Pharmacopsychiatry 17(Suppl 2):59–69
16. Gohlke H, Case DA (2004) Converging free energy estimates: MM-PB(GB)SA studies on the protein-protein complex Ras-Raf. J Comput Chem 25(2):238–250
17. Hou T, Wang J, Li Y, Wang W (2011) Assessing the performance of the MM/PBSA and MM/GBSA methods. 1. The accuracy of binding free energy calculations based on molecular dynamics simulations. J Chem Inf Model 51(1):69–82
18. Everitt AB, Seymour VA, Curmi J, Laver DR, Gage PW, Tierney ML (2009) Protein interactions involving the gamma2 large cytoplasmic loop of GABA(A) receptors modulate conductance. FASEB J 23(12):4361–4369
19. O'Toole KK, Jenkins A (2011) Discrete M3-M4 intracellular loop subdomains control specific aspects of gamma-aminobutyric acid type A receptor function. J Biol Chem 286(44):37990–37999
20. Discovery Studio 3.0 (2011). Accelrys, San Diego, CA
21. Eramian D, Shen MY, Devos D, Melo F, Sali A, Marti-Renom MA (2006) A composite score for predicting errors in protein structure models. Protein Sci 15(7):1653–1666

22. Baumann SW, Baur R, Sigel E (2002) Forced subunit assembly in alpha1beta2gamma2 GABAA receptors. Insight into the absolute arrangement. J Biol Chem 277(48):46020–46025
23. Sigel E, Luscher BP (2011) A closer look at the high affinity benzodiazepine binding site on GABAA receptors. Curr Top Med Chem 11(2):241–246
24. Morris GM, Huey R, Lindstrom W, Sanner MF, Belew RK, Goodsell DS, Olson AJ (2009) AutoDock4 and AutoDockTools4: Automated docking with selective receptor flexibility. J Comput Chem 30(16): 2785–2791
25. AMBER 12 (2012). University of California, San Francisco
26. Wang J, Wolf RM, Caldwell JW, Kollman PA, Case DA (2004) Development and testing of a general amber force field. J Comput Chem 25(9):1157–1174
27. Jakalian A, Jack DB, Bayly CI (2002) Fast, efficient generation of high-quality atomic charges. AM1-BCC model: II. Parameterization and validation. J Comput Chem 23(16):1623–1641
28. Berendsen HJC, Postma JPM, van Gunsteren WF, DiNola A, Haak JR (1984) Molecular dynamics with coupling to an external bath. J Chem Phys 81(7):3684–3693
29. Darden T, York D, Pedersen L (1993) Particle mesh Ewald: An N. log(N) method for Ewald sums in large systems. J Chem Phys 98(12):10089–10092
30. Kräutler V, van Gunsteren WF, Hünenberger PH (2001) A fast SHAKE algorithm to solve distance constraint equations for small molecules in molecular dynamics simulations. J Comput Chem 22(5):501–508
31. Onufriev A, Bashford D, Case DA (2004) Exploring protein native states and large-scale conformational changes with a modified generalized born model. Proteins 55(2):383–394
32. Luu T, Cromer B, Gage PW, Tierney ML (2005) A role for the 2' residue in the second transmembrane helix of the GABA A receptor gamma2S subunit in channel conductance and gating. J Membr Biol 205(1):17–28
33. Gonzales EB, Bell-Horner CL, Dibas MI, Huang RQ, Dillon GH (2008) Stoichiometric analysis of the TM2 6' phenylalanine mutation on desensitization in alpha1beta2 and alpha1beta2gamma2 GABA A receptors. Neurosci Lett 431(2):184–189
34. Horenstein J, Wagner DA, Czajkowski C, Akabas MH (2001) Protein mobility and GABA-induced conformational changes in GABA(A) receptor pore-lining M2 segment. Nat Neurosci 4(5):477–485
35. Pritchett DB, Seeburg PH (1990) Gamma-aminobutyric acidA receptor alpha 5-subunit creates novel type II benzodiazepine receptor pharmacology. J Neurochem 54(5):1802–1804
36. Sancar F, Ericksen SS, Kucken AM, Teissere JA, Czajkowski C (2007) Structural determinants for high-affinity zolpidem binding to GABA-A receptors. Mol Pharmacol 71(1):38–46
37. Hanson SM, Morlock EV, Satyshur KA, Czajkowski C (2008) Structural requirements for eszopiclone and zolpidem binding to the gamma-aminobutyric acid type-A (GABAA) receptor are different. J Med Chem 51(22):7243–7252
38. Teissere JA, Czajkowski C (2001) A (beta)-strand in the (gamma)2 subunit lines the benzodiazepine binding site of the GABA A receptor: structural rearrangements detected during channel gating. J Neurosci 21(14):4977–4986
39. Davies M, Bateson AN, Dunn SM (1998) Structural requirements for ligand interactions at the benzodiazepine recognition site of the GABA(A) receptor. J Neurochem 70(5):2188–2194
40. Ogris W, Poltl A, Hauer B, Ernst M, Oberto A, Wulff P, Hoger H, Wisden W, Sieghart W (2004) Affinity of various benzodiazepine site ligands in mice with a point mutation in the GABA(A) receptor gamma2 subunit. Biochem Pharmacol 68(8):1621–1629
41. Buhr A, Sigel E (1997) A point mutation in the gamma2 subunit of gamma-aminobutyric acid type A receptors results in altered benzodiazepine binding site specificity. Proc Natl Acad Sci USA 94(16): 8824–8829
42. Sigel E, Schaerer MT, Buhr A, Baur R (1998) The benzodiazepine binding pocket of recombinant alpha1beta2gamma2 gamma-aminobutyric acidA receptors: relative orientation of ligands and amino acid side chains. Mol Pharmacol 54(6):1097–1105
43. Castellano S, Taliani S, Milite C, Pugliesi I, Da Pozzo E, Rizzetto E, Bendinelli S, Costa B, Cosconati S, Greco G, Novellino E, Sbardella G, Stefancich G, Martini C, Da Settimo F (2012) Synthesis and biological evaluation of 4-phenylquinazoline-2-carboxamides designed as a novel class of potent ligands of the translocator protein. J Med Chem 55(9):4506–4510
44. Chambon JP, Perio A, Demarne H, Hallot A, Dantzer R, Roncucci R, Biziere K (1985) Ethyl loflazepate: a prodrug from the benzodiazepine series designed to dissociate anxiolytic and sedative activities. Arzneimittelforschung 35(10):1573–1577
45. Dubinsky B, Vaidya AH, Rosenthal DI, Hochman C, Crooke JJ, DeLuca S, DeVine A, Cheo-Isaacs CT, Carter AR, Jordan AD, Reitz AB, Shank RP (2002) 5-ethoxymethyl-7-fluoro-3-oxo-1,2,3, 5-tetrahydrobenzo[4,5]imidazo[1,2a]pyridine-4 -N-(2-fluorophenyl)carboxamide (RWJ-51204), a new nonbenzodiazepine anxiolytic. J Pharmacol Exp Ther 303(2):777–790
46. Fujimoto M, Hirai K, Okabayashi T (1982) Comparison of the effects of GABA and chloride ion on the affinities of ligands for the benzodiazepine receptor. Life Sci 30(1):51–57
47. Vinkers CH, Korte-Bouws GA, Torano JS, Mirza NR, Nielsen EO, Ahring PK, de Jong GJ, Olivier B (2010) The rapid hydrolysis of chlordiazepoxide to demoxepam may affect the outcome of chronic osmotic minipump studies. Psychopharmacology (Berl) 208(4):555–562